SANDIA REPORT
SAND2024-03098
Printed March 2024

Sandia National Laboratories

A Review of Parameter Ranges for Uncertainty Estimation for Decomposing Carbon Fiber Epoxy Composites

Sarah N. Scott

Issued by Sandia National Laboratories, operated for the United States Department of Energy by National Technology & Engineering Solutions of Sandia, LLC.

Available to DOE and DOE contractors from
U.S. Department of Energy
Office of Scientific and Technical Information
P.O. Box 62
Oak Ridge, TN 37831

Telephone: (865) 576-8401
Facsimile: (865) 576-5728
E-Mail: reports@osti.gov
Online ordering: http://www.osti.gov/scitech

Available to the public from
U.S. Department of Commerce
National Technical Information Service
5301 Shawnee Rd
Alexandria, VA 22312

Telephone: (800) 553-6847
Facsimile: (703) 605-6900
E-Mail: orders@ntis.gov
Online order: https://classic.ntis.gov/help/order-methods/

ABSTRACT

Carbon fiber epoxy composites are increasingly used in systems requiring a material that is both strong and light weight, as in airplanes, cars, and pressure vessels. In fire environments, carbon fiber epoxy composites are a fuel source subject to oxidation. This literature review seeks to provide material properties as well as uncertainty bounds for those properties for computational models of decomposing carbon fiber epoxy composites. The goal is to guide analysts when measurements are lacking and increase credibility of uncertainty quantification ranges.

ACKNOWLEDGEMENTS

I would like to acknowledge Matthew Kury and John Hewson for their discussions involving this work, and Raquel Hakes Weston-Dawkes and Camron Proctor for reviewing the document.

CONTENTS

LIST OF FIGURES

LIST OF TABLES

This page left blank

ACRONYMS AND TERMS

Acronym/Term	Definition
UQ	Uncertainty Quantification
TGA	Thermogravimetric Analysis
DSC	Differential Scanning Calorimetry

1. INTRODUCTION

Fiber reinforced plastics are an attractive engineering material due to their low weight to strength ratio. They have been extensively used in automotive and aeronautical industries, as well as other industries where a light weight, yet strong, material is advantageous. However, unlike more traditional engineering materials like metals, fiber reinforced plastics can be a source of fuel in a fire. At temperatures as low as 250°C, epoxies can start to pyrolyze, generating flammable gases. In order to understand the safety risks associated with these materials, it is necessary to understand their behavior when exposed to heating.

Researchers have been studying fiber reinforced plastics for the past four decades. In the 1970s and 1980s, researchers were first understanding the mechanical effects of the structure of the composite, for example, how using woven fabrics compared to using chopped fibers [1, 2]. Experimental programs attempted to answer questions revolving around the minimum flux for ignition and the extinction characteristics of these new materials [3], as well as how they would perform under high heat fluxes [4]. 1D models were created to understand thermal [5, 6] and thermo-mechanical [7] responses of composites when exposed to heat sources. These models required a range of material properties to be measured [8, 9], particularly those involving characterizing the thermal decomposition of the material [10, 11].

While this early research began to answer fundamental questions about the fire safety of fiber reinforced plastics, the number of these sorts of plastics have increased exponentially in the intervening years, as have experimental and computational techniques. Experimental programs have used the cone calorimeter to obtain the minimum heat flux for piloted ignition [12-14], investigated how different epoxy and fiber types affect ignition [15, 16], explored the effects of the thickness of the sample [17], and determined how the percentage of fibers to polymer affects flammability [18]. Other researchers have investigated how flame spread is affected by the presence of high conductivity directional fibers [19].

There has also been a push to better understand the decomposition mechanism for these materials. This typically includes using thermogravimetric analysis (TGA) to track mass loss vs temperature (at a specified heating rate) and differential scanning calorimetry (DSC) to monitor heat flux vs temperature. TGA gives researchers insight into the reaction mechanism, while DSC gives information about the specific heat and heat of reaction [20]. Early work used a graphical method to determine the activation energy and pre exponential factor by plotting the mass loss vs the inverse of temperature [21]. More advanced analytical methods have also been used [12, 22]. As computational availability has increased, the preferred methodology for fitting TGA data has been to use an optimization algorithm [23-26]. The sensitivity of the reaction parameters to the mass loss curve has also been considered [27]. In order to fully understand the reaction mechanism, it is also important to evaluate the composition of the evolved gases [14, 23, 28].

A number of 1D [29] and higher dimensional [24, 30-36] thermal decomposition models have been created for fiber reinforced plastics. These higher fidelity models require an increasing number of material properties in order to solve the constituent equations [36-46]. These material properties include, but are not limited to, conductivity, density, specific heat, permeability, and emissivity. These properties need to be measured for not only the virgin state of the material, but also at the intermediate decomposed states. In addition, many composites are made up of fabrics that introduce anisotropy into the material properties, particularly the conductivity and the permeability. Further complicating the problem, many models are formulated on a species basis (i.e., epoxy, carbon fiber, char…) making it even more difficult to specify the material properties, particularly if the

composition of the composite is unknown due to the proprietary nature. This problem only increases when the thermo-mechanical problem is considered [33, 34, 47-52].

In this work, I will review the literature to provide material properties with uncertainty bounds for computational models of decomposing carbon fiber epoxy composites. First, I will review the equation set used in our computational model, then review literature for each of the material properties for each of the properties needed for the model. The goal of this work is to provide analysts material properties with appropriate values and bounds when preforming a UQ analysis with a composite material. Recommended values are labeled as 'this study' in the proceeding review. Anytime measurements can be taken of a specific composite of interest, that should supersede this study.

The literature for reaction mechanisms will be reviewed, however no mechanism will be recommended, nor will a way to vary these parameters be suggested. The reaction parameters are highly coupled, causing issues when varying these parameters as scalars. In reviewing the literature, there was not an established way to deal with these parameters. As it is a current research topic, I point the interested reader to Frankel *et al.* [53] to learn more about parameter ranges for carbon fiber epoxy composites through Bayesian analysis. For additional experimental TGA results, I recommend Hakes *et al.* [54].

2. COMPUTATIONAL MODEL DESCRIPTION

1.1. General Numerical Description

The pyrolysis and smolder of the carbon fiber epoxy composite is computationally modeled using the Sierra Thermal/Fluids code, Aria, a multiphysics finite element code created at Sandia National Laboratories [55]. The composite is modeled as a porous medium, which is comprised of two phases, a solid matrix phase and a gaseous fluid phase. Each phase is represented as a mixture model of its constituent parts, and the two phases interact though changes in their relative volume and the exchange of mass and heat. In the following description Latin superscript letters will be used to indicate phase and species, subscripted Latin letters used to indicate specific conditions of the variable, with the letters i and j reserved to represent coordinate indices.

An important derived property in the porous equations is the porosity. The porosity is the ratio of the volume occupied by the gas phase over the total volume. The function form of the porosity is:

$$\phi = \frac{V^g}{V_{total}} = 1 - \frac{V^s}{V_{total}} \tag{1}$$

Where ϕ is the porosity, V^g is the volume occupied by gaseous material, V^s is the volume occupied by solid material, and V_{total} is the total volume of the sample. Porosity transforms physical parameters from their phase volume average to their total or bulk average values. The solid and gas phase bulk density is obtained by:

$$\rho_b^s = (1-\phi)\rho^s \tag{2}$$

$$\rho_b^g = \phi\rho^g \tag{3}$$

where ρ_b^s is the solid phase bulk density, ρ_b^g is the gas phase bulk density, ρ^s is the solid phase's phase density (the mass of the solid material over the volume occupied by the solid material), and ρ^g is the gas phase's phase density.

2.1.1. Gas Phase Equations

In the gas phase, the continuity, species, and enthalpy equations are solved. Darcy's law is used to approximate the flow of the gases. Gases are allowed to enter and exit the domain at specified boundaries. In this formulation, in the continuity equation density is related to pressure through the ideal gas law to solve the gas pressure. In the condensed phase, the species and enthalpy equations are solved, and the two phases are coupled through source terms in the species equations and a volumetric heat transfer term in the enthalpy equations. This derivation is based on the model by Lautenberger *et al.* [56].

The porous gas phase continuity equation is:

$$\frac{\partial(\phi\rho^g)}{\partial t} + \frac{\partial\left(\rho^g u_i^g\right)}{\partial x_i} = \sum_k \dot{\omega}_{bf}^{gk} - \dot{\omega}_{bd}^{gk} \tag{4}$$

where $\dot{\omega}_{bf}^{gk}$ and $\dot{\omega}_{bd}^{gk}$ are the bulk formation and destruction rate of gas phase mass for the k^{th} gas species, ρ^g is the gas density, and u_i^g is the bulk velocity in direction i of the gas. The advective term in this equation does not explicitly have the porosity shown, this is because the porosity is implicitly represented though the bulk velocity. The bulk velocity is represented using the Darcy approximation, which approximates the momentum equation:

$$u_i^g = -\frac{1}{\mu^g}\overline{K}_{ij}\left(\frac{\partial p^g}{\partial x_j} + \rho^g g_j\right) \tag{5}$$

where $\overline{K}$ is the mixture averaged solid phase permeability tensor, μ^g is the gas phase viscosity and g is the gravity vector. The ideal gas law is used to relate the pressure to the density

$$\rho^g = \frac{\overline{M}p^g}{RT^g} \tag{6}$$

where $\overline{M}$ is the mass averaged molecular weight, R is the gas constant, and T^g is the gas temperature. (4), (5), and (6) are combined to give the form of porous gas phase continuity-momentum equation:

$$\frac{\partial}{\partial t}\left(\frac{\overline{M}p^g\phi}{RT^g}\right) + \frac{\partial}{\partial x_i}\left(\frac{\overline{M}p^g}{RT^g}\frac{\overline{K}_{ij}}{\mu^g}\left(\frac{\partial \rho^g}{\partial x_j} + \frac{\overline{M}p^g}{RT^g}g_j\right)\right) = \sum_k \dot{\omega}_{bf}^{gk} - \dot{\omega}_{bd}^{gk} \tag{7}$$

The gas phase species is:

$$\frac{\partial(\phi\rho^g Y^{gk})}{\partial t} + \frac{\partial\left(\rho^g u_i^g Y^{gk}\right)}{\partial x_i} = -\frac{\partial q_i^{gk}}{\partial x_i} + \dot{\omega}_{bf}^{gk} - \dot{\omega}_{bd}^{gk} \tag{8}$$

where Y^{gk} is the gas phase mass fraction of the k^{th} species, $\left(\dot{\omega}_{bf}^{gk} - \dot{\omega}_{bd}^{gk}\right)$ is the difference between the formation and destruction rates for gas phase reactions, and q_i^{gk} is the gas phase species diffusion flux, defined as:

$$q_i^{gk} = -\phi\rho^g D_{ij}^{gk}\frac{\partial Y^{gk}}{\partial x_j} \tag{9}$$

where D^{gk} is the gas phase mass diffusivity for the k^{th} species. The gas phase enthalpy is:

$$\frac{\partial\phi\rho^g h^g}{\partial t} + \frac{\partial\rho^g h^g u_i^g}{\partial x_i} = -\frac{\partial\tilde{q}_i^g}{\partial x_i} + \frac{\partial\phi p^g}{\partial t} + C_v\left(T^s - T^g\right) + \sum_k\left(\dot{\omega}_{bf}^{gk} - \dot{\omega}_{bd}^{gk}\right)h^{gk} \tag{10}$$

where h^g is the mixture averaged gas phase enthalpy, C_v is the volumetric heat transfer coefficient, T^s is the solid phase temperature, T^g is the gas phase temperature, h^{gk} is the gas phase enthalpy of the k^{th} species. $\tilde{q}_i^{gk}$ is the gas phase energy flux and is modeled as:

$$\tilde{q}_i^{gk} = -\phi\rho^g D_{ij}^g \frac{\partial h^g}{\partial x_j} \tag{11}$$

where D^g is the mixture averaged gas phase mass diffusivity.

2.1.2. Solid Phase Equations

In the solid phase the same main governing equations present in the gas phase are solved: mass, species, and enthalpy. The main difference between the solid and gas phase versions of these equations is the loss of the advective term, as for this formulation it is assumed that motion in the solid phase is negligible.

The solid phase continuity equation is:

$$\frac{\partial \rho_b^s}{\partial t} = \sum_k \dot{\omega}_{bf}^{sk} - \dot{\omega}_{bd}^{sk} \tag{12}$$

where $\dot{\omega}_{bf}^{s}$ and $\dot{\omega}_{bd}^{sk}$ are the bulk formation and destruction rate of solid phase mass for the k^{th} species, respectively.

The condensed phase species equation is:

$$\frac{\partial\left(\rho_b^s Y^{sk}\right)}{\partial t} = \dot{\omega}_{bf}^{sk} - \dot{\omega}_{bd}^{sk} \tag{13}$$

where $\dot{\omega}_{bf}^{sk} - \dot{\omega}_{bd}^{sk}$ is the difference between the formation and destruction rates of solid phase mass for the k^{th} species and Y^k is the condensed phase mass fraction of the k^{th} species.

The condensed phase enthalpy is defined as:

$$\frac{\partial \rho_b^s T^s c_p}{\partial t} = -\frac{\partial \tilde{q}_j^s}{\partial x_j} + C_v(T^g - T^s) \tag{14}$$

where c_p is the specific heat in the condensed phase and q_j^h is the condensed phase energy flux:

$$\tilde{q}_j^s = -(K_b + K_r)\frac{\partial T^s}{\partial x_j} \tag{15}$$

where K_b is the bulk thermal conductivity and K_r is an effective conductivity for radiant heat transfer in optically thick media.

3. MATERIAL PROPERTIES AND UNCERTAINTY

This section covers the specific representations of several key material parameters present in the governing equations for the porous composite model. In each subsection a material property will be highlighted, its representation in our model detailed, and the spread of experimental evidence related to the parameter discussed. Recommended values will be labeled as 'this study' and bounds on that value will be provided.

3.1. Density

Density is a critical parameter to capture, because of how important the transfer of mass is to the composite decomposition problem. As described in section 1.1, in modeling the composite as a porous medium two scales of density must be defined: the bulk averaged density and the phase averaged density. In addition, the density of a particular phase of the composite is the summation of the different species constituents in that phase. This allows us to define a 'partial bulk density', analogous to what partial pressure represents in a gas mixture. In this case the partial density, ρ_p^k, is defined as:

$$\rho_p^k = \rho_b \, Y^k \tag{16}$$

Where Y^k is the mass fraction of the k^{th} species. Written another way the bulk density is the sum of the partial densities:

$$\rho_b = \sum_k \rho_p^k \tag{17}$$

With the 'partial bulk density' the volume fractions occupied by the solid components ($\mathbb{V}^{sk}$) can be determined:

$$\mathbb{V}^{sk} = \frac{\rho_p^{sk}}{\rho^k} \tag{18}$$

Where ρ^k is the phase average density of the k^{th} species. Any space not occupied by the solid material is assumed to be occupied by the gas phase, thus summing the solid volume fractions the porosity can be determined:

$$\phi = \mathbb{V}^g = 1 - \Sigma \mathbb{V}^{sk} \tag{19}$$

A collection of the experimentally determined densities of carbon fiber composites are shown in Figure 1. These density values provide us with the initial bulk density values for our composite. To use the porous formulation, this overall data needs to be augmented with the densities of the contributing components in isolation. These densities are shown in Figure 1. Of note is the spread in densities of the char. This is due to what people mean by 'char'. For example, McKinnon *et al.* [24] have four values for char represented in the graph. In their work, they stopped the progression of the decomposition at a certain point (*i.e.*, at the end of 'reaction 1') and then measured the properties. The values used in our model are shown in Table 1.

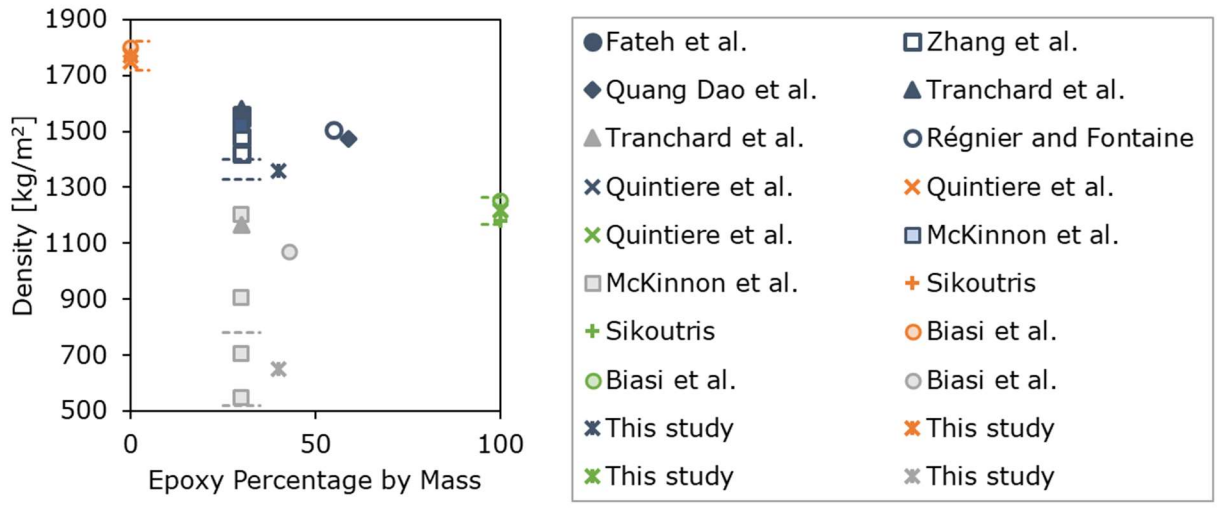

Figure 1: The density of the composite (blue), carbon fiber (orange), epoxy (green), and char (or charred composite) (grey) vs the epoxy percentage by mass.

Table 1: Recommended bulk densities, along with the uncertainty. The uncertainty of the residue is assumed to be the same as the char.

	Density [kg/m³]	*Uncertainty*
Composite	1360	±2.25
Epoxy	1215	±4
Carbon Fiber	1770	±3
Char	650	±20
Residue	650	±20

3.2. Conductivity

The conductivity of a decomposing carbon fiber epoxy composite is not a trivial matter. The composite is made of the two constituent materials, carbon fiber and epoxy. When the decomposition occurs, char is formed and will alter the conductivity. In addition, sheet composites are anisotropic, as carbon fiber has a much higher conductivity than epoxy [18, 30, 33, 34, 51]. This can lead to up to an order of magnitude difference in plane vs out of plane conductivities [18, 34, 36]. Additional complications in determining composite conductivity stem from the variation in the experimental methods used, from the use of hot plate methods to backing out values using time to ignition in a cone calorimeter (or similar apparatus) [15, 17].

For this study, the values for conductivity are listed in Table 2. The uncertainties are based on capturing the spread in the literature for each material. These are shown in Figure 2 alongside values from literature. In our model the conductivity is modeled as the sum of a transverse anisotropic bulk conductivity and an isotropic effective radiation conductivity. Making use of the rule of mixtures, equation (20) is the in-plane bulk conductivity ($K_{b\parallel}$), where $\mathbb{V}^k$ is the volume fraction of the k^{th} component (*e.g.* epoxy, carbon fiber…) and K^k is the component isotropic conductivity. Similarly, equation (21) is the out of plane conductivity ($K_{b\perp}$). Figure 3 shows the volume averaged conductivities and the resulting uncertainties used in this study, along with literature values.

$$K_{b\parallel} = \Sigma \mathbb{V}^k K^k \tag{20}$$

$$\frac{1}{K_{b\perp}} = \sum \frac{\mathbb{V}^k}{K^k} \tag{21}$$

Table 2: Recommended conductivities, along with the uncertainty. For properties varying with temperature, linear interpretation is used between defined points.

	Conductivity [W/mK]				*Uncertainty*
	In Plane		*Out of Plane*		
Epoxy	0.15		0.15		±50%
Carbon Fiber	*Temperature [C]*		*Temperature [C]*		±50%
	0	0.56	0	0.056	
	256	4	256	0.4	
	727	10.62	727	1.062	
Char	0.029		0.0029		-90% + 200%
Residue	7.25e-6		7.25e-6		-90% + 200%

One additional solid component, beyond the epoxy, carbon fiber, and char is included in this study: residue. This is the solid phase product of the oxidation of the carbon fiber. In experiments, this is an ashy material, and thus defining a bulk conductivity for this material is difficult. I am specifying the residue's conductivity to be very low because it is a discontinuous material, and the presence of residue is an indication of the delamination of the composite. These two factors reduce the thermal contact within the material, and when residue is present in the mixture calculation its conductivity needs to capture the additional reduction in conductivity due to the breaking of thermal contact.

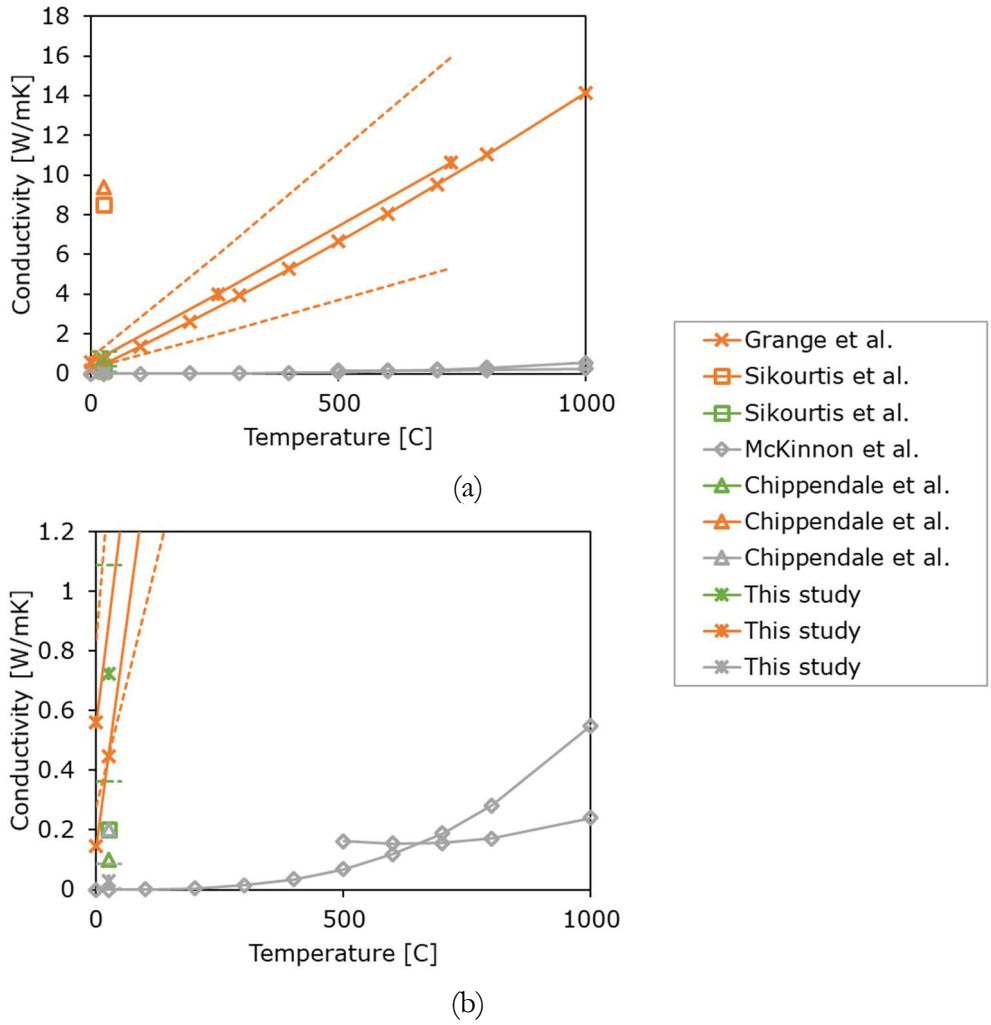

Figure 2: The conductivity of carbon fiber (orange), epoxy (green) and char (or charred composite) (grey) vs temperature. (a) Shows the range of the conductivities while (b) zooms in on the conductivities from 0 to 1.2 W/mK to make the conductivities of the epoxy more visible. The dashed lines are the uncertainty for this study. If a temperature was not given, the data was assumed to be at 25°C in order to plot.

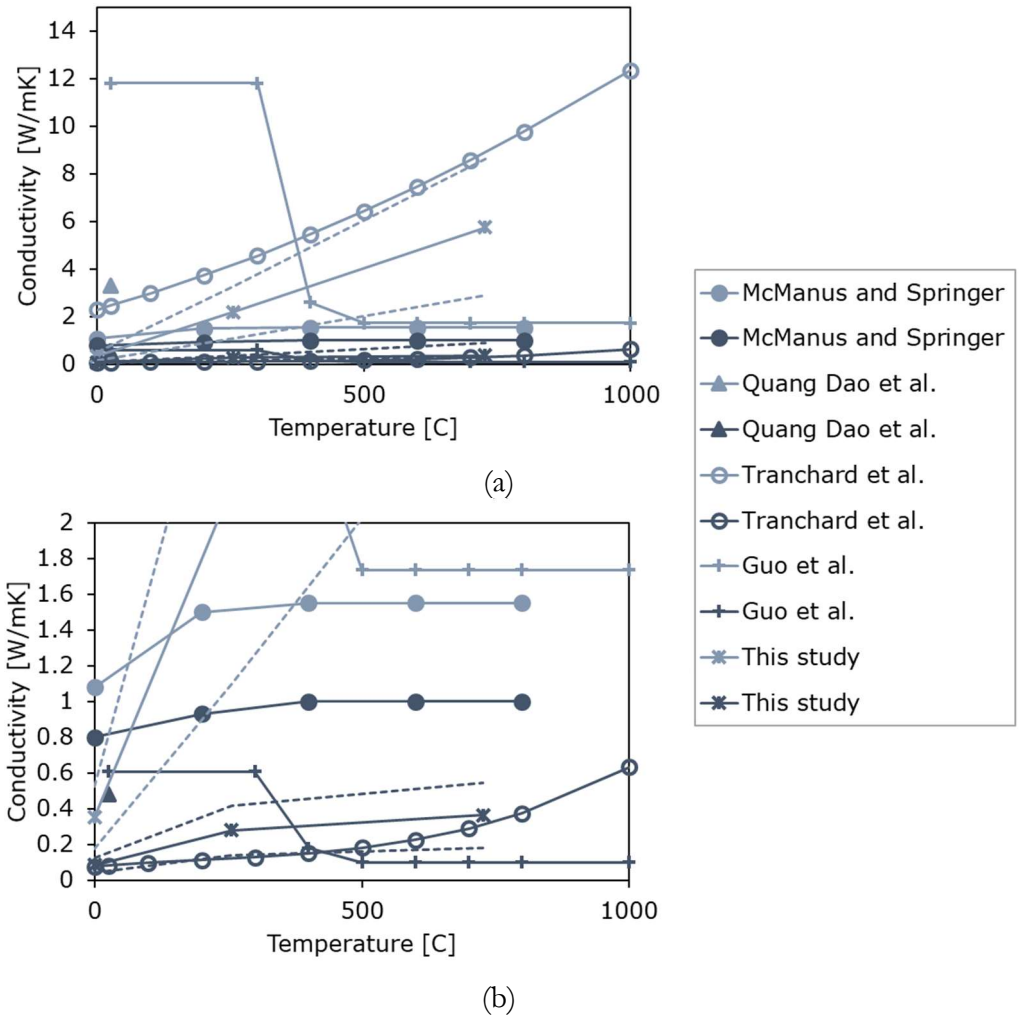

Figure 3: The anisotropic conductivity of carbon fiber epoxy composite in the normal (dark blue) and transverse (light blue) directions vs temperature. (a) Shows the range of the conductivities while (b) zooms in on the conductivities from 0 to 2 W/mK to make the in-plane conductivities visible. The dashed lines are the uncertainty for this study. If a temperature was not given, the data was assumed to be at 25°C. Since the decomposition temperature of epoxy is ~350°C, data higher than that temperature should be considered to be of a partially decomposed composite. The values for this study were calculated using the inputs from Table 2 and calculated using (20) and (21).

In the literature, particularly for cases where the conductivity was ascertained from the time to ignition, a singular value for the conductivity is reported for the composite. These values are shown in Figure 4.

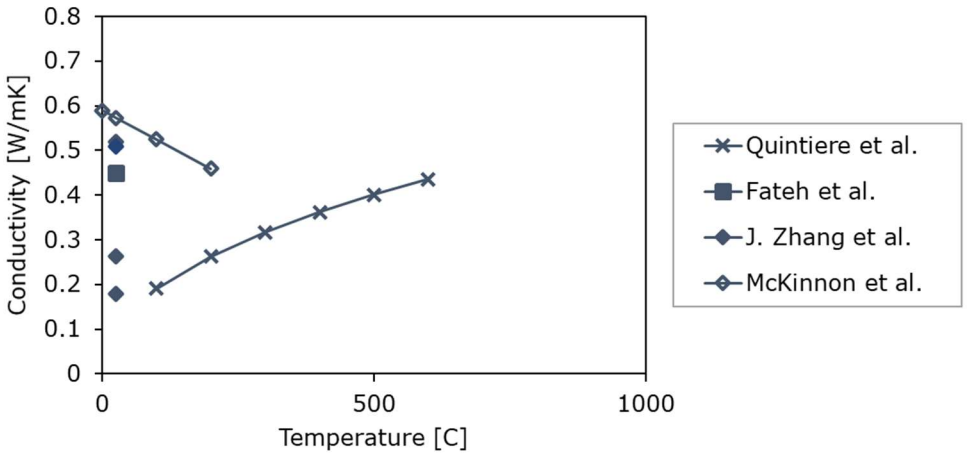

Figure 4: The isotropic conductivity of carbon fiber epoxy vs temperature. If a temperature was not given, the data was assumed to be at 25°C. Since the decomposition temperature of epoxy is ~350°C, data higher than that temperature should considered as a partially decomposed composite. Our study is not shown on this plot, as our material is modeled as an anisotropic material.

3.3. Specific Heat

The specification of the solid phase specific heat is modeled as a volume average mixture of the component specific heats.

$$c_p = \Sigma \mathbb{V}^{\mathrm{k}}\, c_p^k \tag{22}$$

Researchers have investigated the specific heat of carbon fiber epoxy composites as a function of the constituents and as a composite. Figure 5 gives values for the carbon fiber alone, Figure 6 gives values for the char, and Figure 7 gives values for the epoxy. Figure 8 gives values for researchers who measured the specific heat of the combined composite.

Sikoutris *et al.* [51] measured the properties for a carbon fiber epoxy composite that was 50% by mass fiber. They gave values for the carbon fiber and epoxy separately. Chippendale *et al.* [35] also investigated a carbon fiber epoxy composite, reporting values for the fiber, epoxy, and char. Grange *et al.* [57] reported measurements for a carbon PEKK (Polyetherketoneketone) and a carbon phenolic composite. They reported values as a function of temperature for the fiber, resin, and char. Dimitrienko [50] measured the properties for a glass fiber epoxy composite and reported values for the fiber, the epoxy and the char.

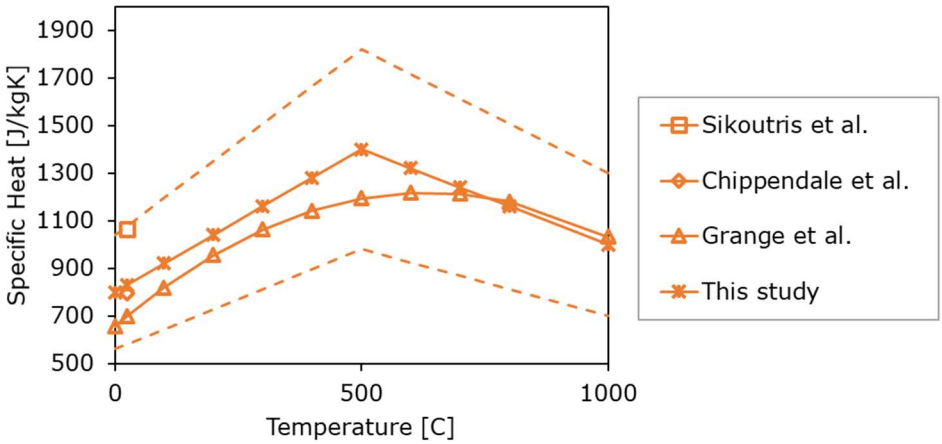

Figure 5: The specific heat of carbon fiber vs temperature. The dashed lines are the uncertainty for this study. If a temperature was not given, the data was assumed to be at 25°C.

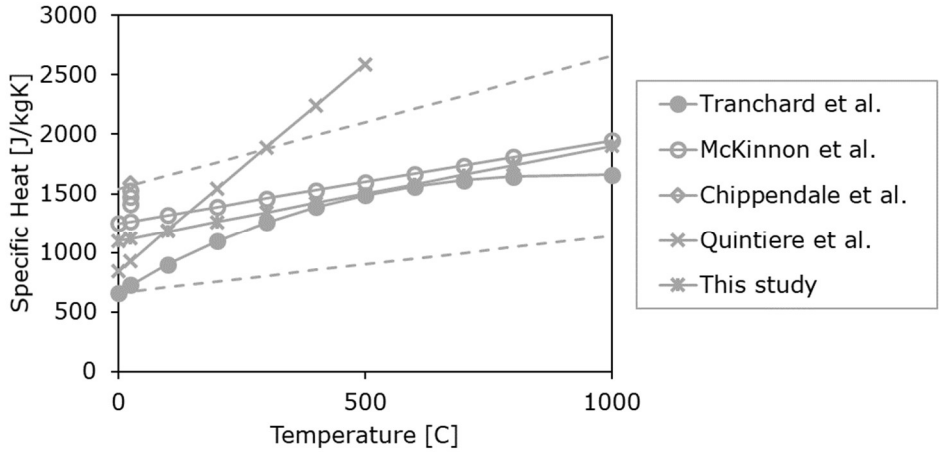

Figure 6: The specific heat of char (or charred composite) vs temperature. The dashed lines are the uncertainty for this study. If a temperature was not given, the data was assumed to be at 25°C.

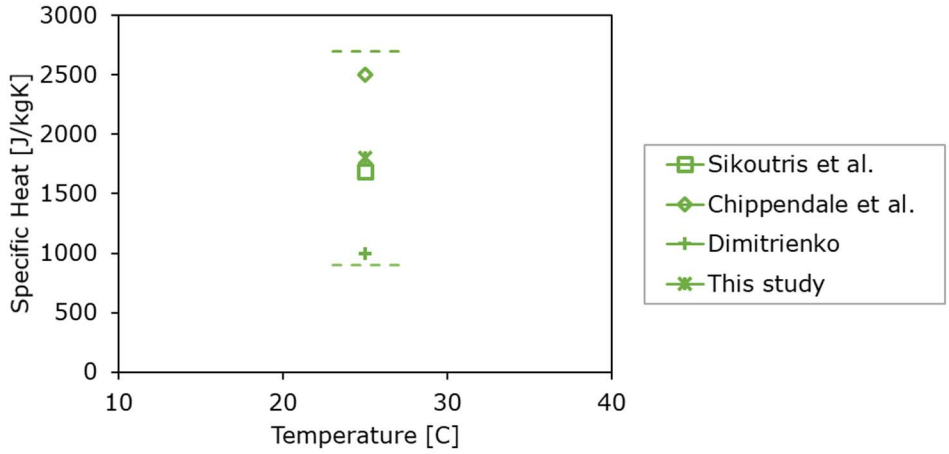

Figure 7: The specific heat of epoxy vs temperature. The dashed lines are the uncertainty for this study. If a temperature was not given, the data was assumed to be at 25°C.

Tranchard *et al.* [33] measured the measured the values for a composite that was 30% epoxy by mass, and reported values for the mixed composite, as well as the char, all as a function of temperature. McKinnon *et al.* [24] also measured values for the composite material, as well as the char at four intermediate stages. While the virgin material was reported as a function of temperature, the char material was not. Quintiere *et al.* [12] reported values for the composite and the char, both as a function of temperature.

Many researchers measured only the virgin composite. Fateh *et al.* [17] reported values for a composite that was 30% by mass epoxy. Zhang *et al.* [15] used time to ignition with three types of carbon fiber epoxy composites (each 30% by mass epoxy) to determine the specific heat. Quang Dao *et al.* [18] measured a singular value for the specific heat for a composite that was 59% fiber by volume while Guo [36] presented a table of values for their composite, ranging from 25C to 3316C.

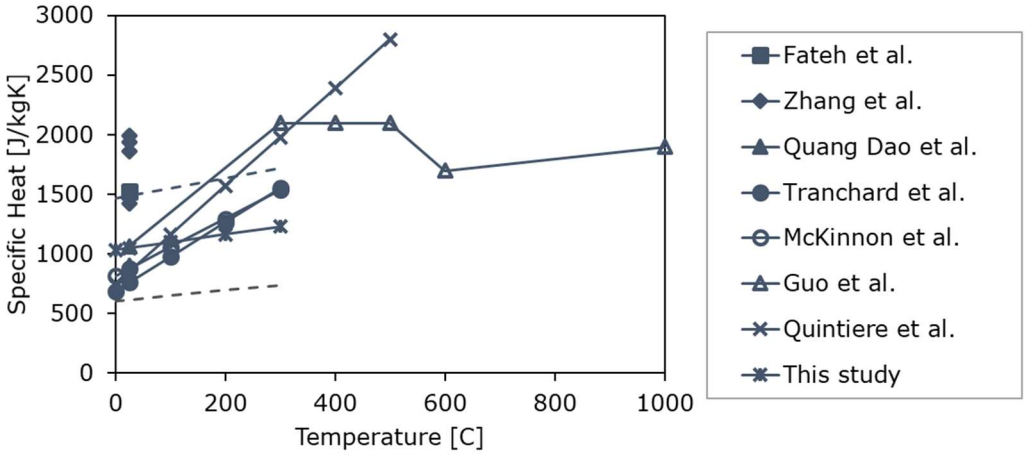

Figure 8: The specific heat of carbon fiber epoxy composite vs temperature. The dashed lines are the uncertainty for this study. If a temperature was not given, the data was assumed to be at 25°C. Since the decomposition temperature of epoxy is ~350°C, data higher than that temperature should be considered to be of a partially decomposed composite. The values for this study were calculated using the inputs from Table 3 and calculated using (22).

Table 3: Specific heats used in this study, along with the uncertainty. For properties varying with temperature, linear interpretation is used between defined points.

	Specific Heat [J/kgK]		*Uncertainty*
Epoxy	1800		±50%
Carbon Fiber	*Temperature [C]*		±30%
	0	800	
	500	1400	
	1000	1000	
Char	*Temperature [C]*		±40%
	0	800	
	500	1500	
	1000	1900	
Residue	850		±40%

3.4. Permeability

The permeability of the composite will change over time as the material degrades. Sullivan [58], Goodrich [39], and Golestanian [40] all measured the permeability as a function of the decomposition. Sullivan measured it for a virgin and a charred sample; Goodrich as a function of mass loss; and Golestanian as a function of porosity. With the information given in the papers, there wasn't a way to convert these measured values to something uniform to compare against. Therefore, Figure 9 presents the permeability data as a range, where blue is the virgin sample and grey is the charred sample. McManus et al. [59] took the additional step of measuring the anisotropic permeability (as a function of char volume). In a layer composite, as the epoxy decomposes, the gases preferentially flow along the layers of carbon fiber, as that is the path of least resistance. To reflect this, the composite is more permeable in the in-plane direction. Along with the literature data, Figure 9 shows the values used in this work, which are also tabulated in Table 4. As with all the material properties, they must be defined for each species of the composite. These properties are volume averaged using the same volume averaging scheme as the specific heat (Equation (22)). The virgin permeability of the composite is also shown in Figure 7.

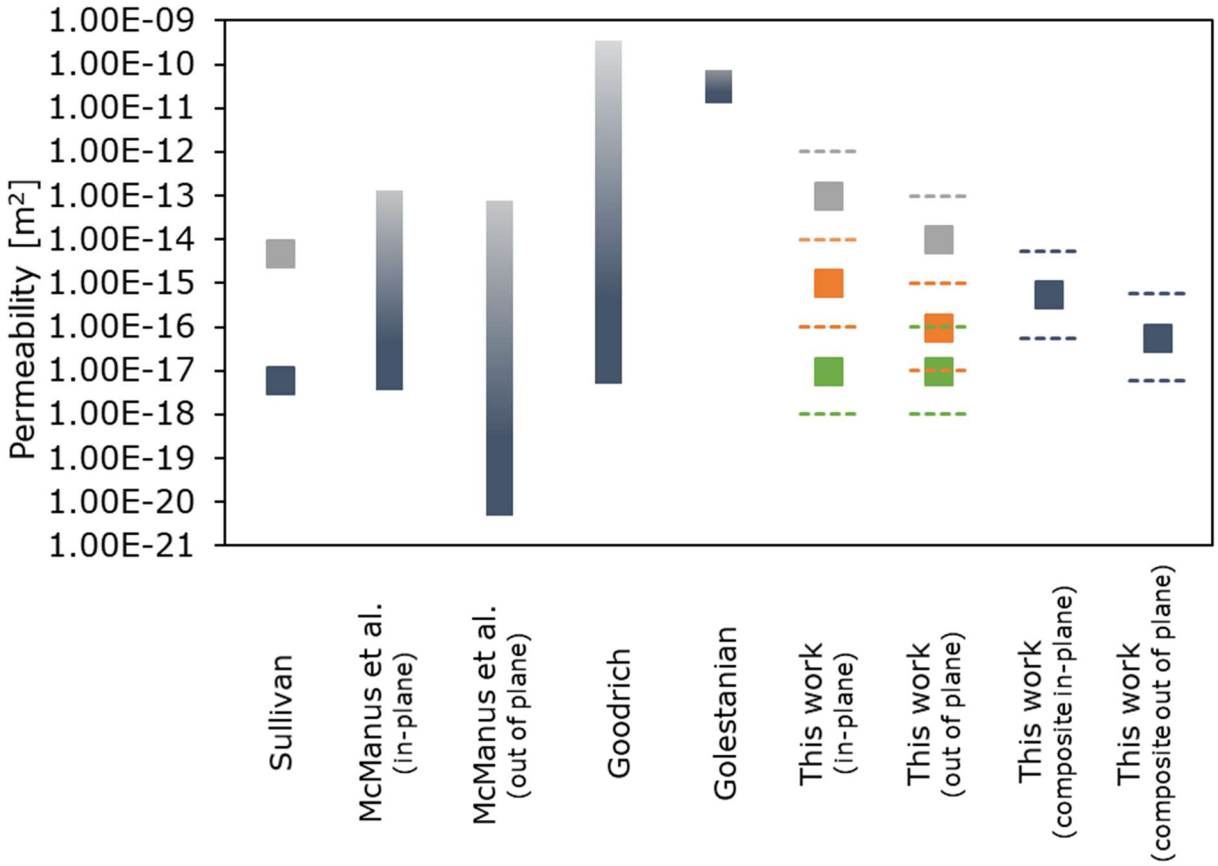

Figure 9: The permeability of the composite. Blue indicates virgin composite, grey indicates char, orange is carbon fiber and green in epoxy. In our model, the material properties are specified by phase (carbon fiber, epoxy, char). The composite values for our work are calculated from those and shown for reference. The dashed lines are the uncertainty for this study.

Table 4: Permeability used in this study, along with the uncertainty.

	Permeability [m^2]		*Uncertainty*
	In Plane	*Out of Plane*	
Epoxy	1E-17	1E-17	-90% +900%
Carbon Fiber	1E-15	1E-16	-90% +900%
Char	1E-13	1E-14	-90% + 200%
Residue	1E-13	1E-14	-90% + 200%

3.5. Radiative Conductivity

For this study, heat transferred through the pore space is approximated by adding an effective conductivity for radiant heat transfer (K_r in equation (15)). The conductivity can be approximated as:

$$K_r = \frac{16}{3\beta_R}\sigma T^3 \tag{23}$$

where β_R is the Rosseland-mean extinction coefficient, σ is the Stefan-Boltzmann constant, and T is the temperature. The Rosseland-mean extinction coefficient can be measured, and has been for carbon fiber epoxy composites [41], phenolic foam insulation [42], and alumina-silica fibrous insulation [43]. Van Eekelen et al. offer an alternative way to calculate the effective conductivity for a carbon fiber epoxy composite based on the geometry of the material [44]. The effective conductivity from each paper, along with value used in this work, are shown in Figure 10. In this case, I used the same value for each species of the composite.

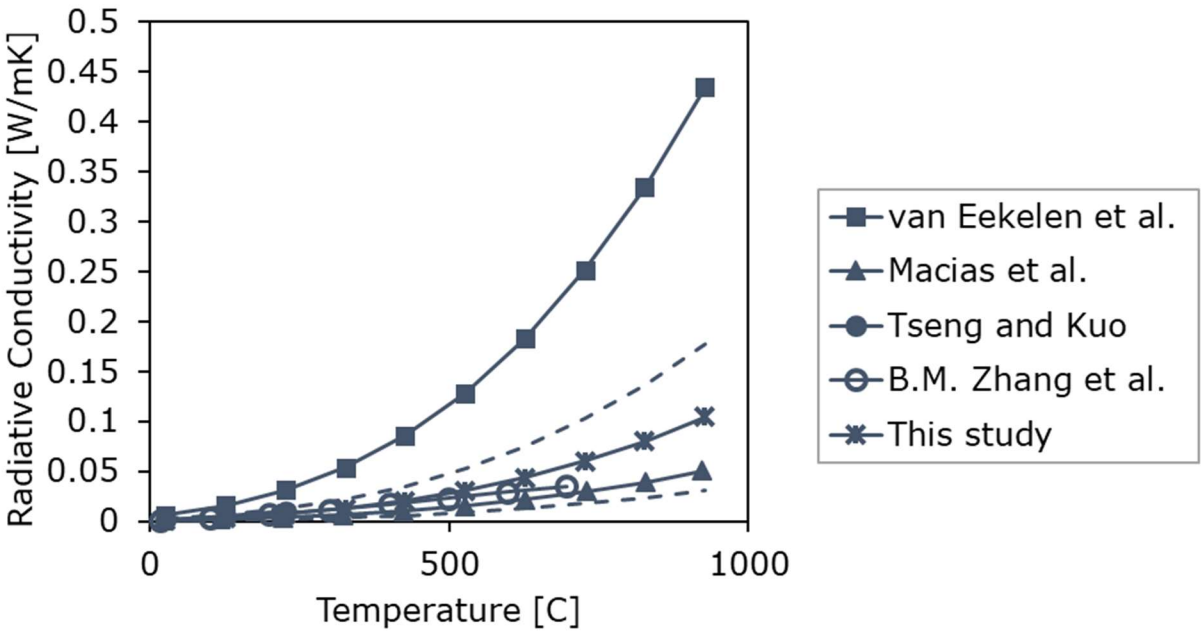

Figure 10: The effective conductivity from literature, shown with value used in this work. The dashed lines are the bounds of the uncertainty.

Table 5: Effective conductivity used in this study, along with the uncertainty.

	Radiative Conductivity [W/mK]	*Uncertainty*
Composite	$\frac{16}{(3*5000)\sigma T^3}$	±70%

3.6. Emissivity

As with the radiative conductivity, the emissivity is specified for the composite, rather than for each species. Several researchers have measured the emissivity of the virgin composite. Pouliot Laforte *et al.* [45] measured the emissivity up to 100°C (which is below the decomposition temperature). Adibekyan *et al.* [46] presented a range for their measurement, which span 0.15. Sullivan [58] measured both the virgin and char emissivity; both values were within the range that Adibekyan *et al.* published. As such, I chose to not assign a different value for the components. Figure 11 shows these literature values, along with the value used in this study.

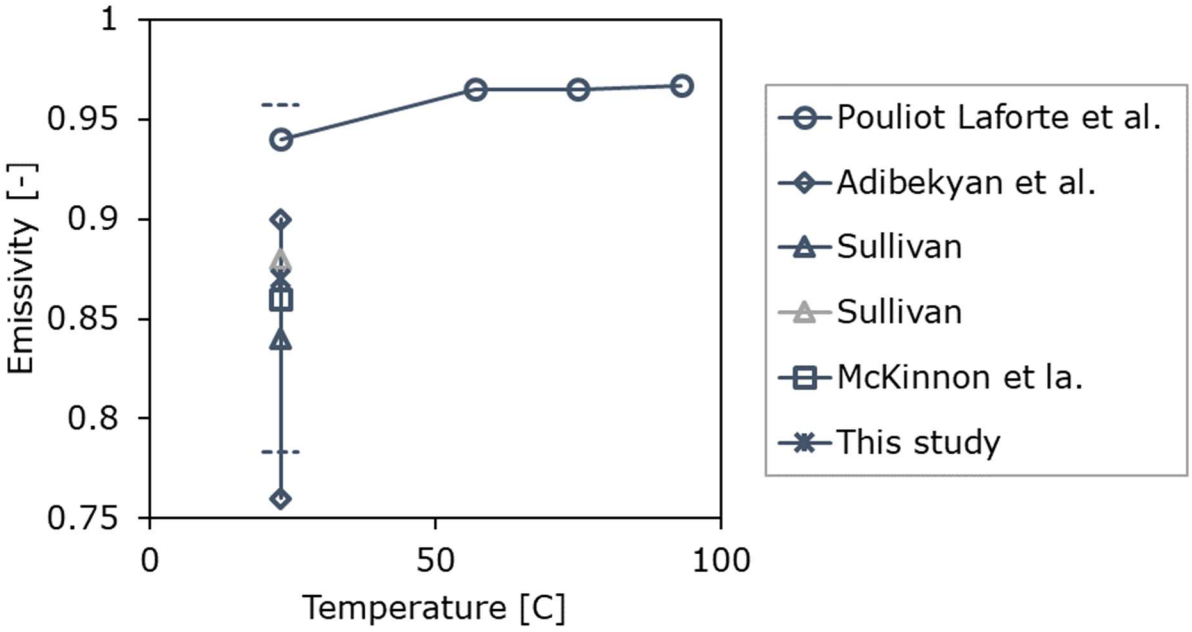

Figure 11: The emissivity from literature, shown with value used in this work. The dashed lines are the bounds of the uncertainty.

Table 6: Effective emissivity used in this study, along with the uncertainty.

	Radiative Conductivity [W/mK]	*Uncertainty*
Composite	0.87	±10%

3.7. Reactions

As discussed in the introduction, only the literature for reaction mechanism will be discussed. A mechanism will not be recommended, nor will ranges be provided. Determining a suitable reaction is more difficult that assigning most other material properties. The parameters are coupled, leading to unphysical results if each component is varied independently. This is a current research topic, so I suggest you see our work Frankel *et al.* [53] for possible fits and Bayesians analysis and ranges and

Hakes *et al.* [54] for additional experimental data. Recommendations for fits and parameter ranges will be left to future work.

When determining a reaction for a composite, it is necessary to understand the behavior in both inert and oxygenated environments. Plots of the mass loss from select mechanisms is shown in Figure 12 and the parameters from the fits are shown in Table 7. Fateh *et al.* [17], McKinnon *et al.* [24], and Quintiere *et al.* [12] developed reactions in inert environments. Fateh *et al.* and Quintiere *et al.* both used a one-step reaction, while McKinnon *et al.* developed a four-step reaction. The four-step reactions smooths the transition from the composite mass loss to the residual mass. Biasi *et. al.* [26] and Branca *et. al.* [25] both developed mechanisms for oxidizing environments. In both cases a three-step mechanism was used.

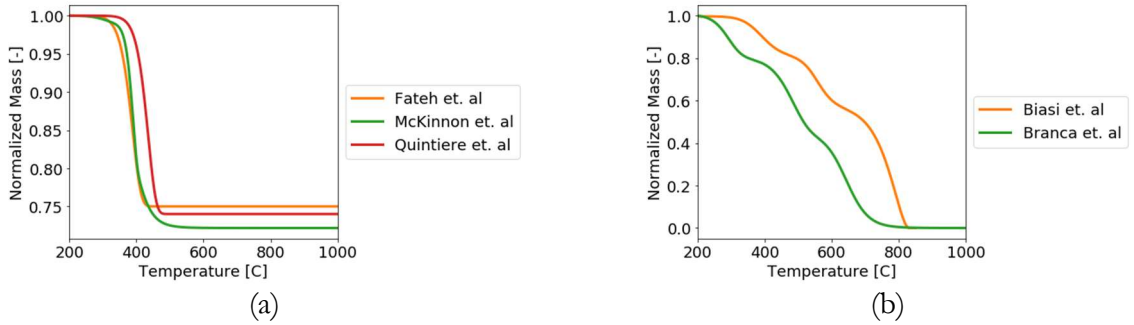

Figure 12: Normalized mass loss vs temperature for TGA from the literature for (a) inert and (b) oxidative conditions.

Table 7: Kinetic parameters from literature

		Inert			Oxidative		
	Rxn	A [1/s]	E [kJ/mol]	n [-]	A [1/s]	E [kJ/mol]	n [-]
Ragnier	1	121	92	1	8.04e6	132	1
	2	24	103	1	3.28e5	154	1
	3	-	-	-	3.32	108	1
Quintiere	1	9.67e10	182	1	-	-	-
Tranchard	1	7.2	58.7	1.11	-	-	-
	2	5.33e8	146.7	2.08	-	-	-
Fateh	1	1.97e9	149	1	-	-	-
Branca	1	1.4e4	82	1.25	1.4e5	82	1.25
	2	1.1e4	90.5	1.6	3.2e4	104.6	1.07
	3	-	-	-	1.2e8	184	1.75
Biasi	1	4.18e10	164	2.72	9.03e5	106	1.8
	2	-	-	-	5.65e10	203	1.8
	3	-	-	-	2e5	167	0.5
McKinnon		$\left[\frac{(m^3/kg)^{n-1}}{s}\right]$	[kJ/mol]	[-]	$\left[\frac{(m^3/kg)^{n-1}}{s}\right]$	[kJ/mol]	[-]
	1	4.09e5	91.8	1	-	-	-
	2	6.16e19	278	1	-	-	-
	3	1.23e21	301	1	-	-	-
	4	150	8e5	2	-	-	-

4. CONCLUSION

This work has presented an extensive literature review for the material properties needed to populate a porous media model for a carbon fiber epoxy composite. Along with nominal values (should experimental measurements be lacking), appropriate ranges, based on the spread in the literature values, are provided. The goal of this work is to guide analysis when implementing a decomposing composites model, as well as provide credibility for ranges in uncertainty quantification studies.

Left to future work is an in-depth analysis of a best practice for applying uncertainty ranges to decomposition mechanisms. This work was started in Frankel *et al.* [53] and will continue in the future.

REFERENCES

[1] T. Ishikawa and T. W. Chout, "One-dimensional micromechanical analysis of woven fabric composites," *AIAA Journal,* vol. 21, no. 12, pp. 1714-1721, 1983, doi: 10.2514/3.8314.

[2] P. T. Curtis and S. M. Bishop, "An assessment of the potential of woven carbon fibre-reinforced plastics for high performance applications," *Composites,* vol. 15, no. 4, pp. 259-265, October 1984 1984, doi: 10.1016/0010-4361(84)90706-7.

[3] J. E. Brown, E. Braun, and W. H. Twilley, "Cone Calorimeter Evaluation of the Flammability of Composite Materials," US Department of Commerce, National Bureau of Standards, Gaithersburg, MD, 1988, vol. NSBIR 88-3733.

[4] J. P. Fanucci, "Thermal Response of Radiantly Heated Kevlar and Graphite/Epoxy Composites," *Journal of Composite Materials,* vol. 21, no. 2, pp. 129-139, 1987, doi: 10.1177/002199838702100204.

[5] J. B. Henderson, J. A. Wiebelt, and M. R. Tant, "A Model for the Thermal Response of Polymer Composite Materials with Experimental Verification," *Journal of Composite Materials,* vol. 19, no. 6, pp. 579-595, 1985, doi: 10.1177/002199838501900608.

[6] J. B. Henderson and T. E. Wiecek, "A Mathematical Model to Predict the Thermal Response of Decomposing, Expanding Polymer Composites," *Journal of Composite Materials,* vol. 21, no. 4, pp. 373-393, 1987, doi: 10.1177/002199838702100406.

[7] C. I. Chang, "The Effects on Polymer Composite Structures," *Theoretical and Applied Fracture Mechanics,* vol. 6, pp. 113-120, 1986.

[8] W. A. Clayton, "Constituent and Composite Thermal Conductivities Of Phenolic-Carbon A N D Phenolic-Graphite Ablators," in *AIAA/ASME 12th Structures, Structural Dynamics, and Materials Conference*, Anaheim, CA, April 19-21, 1971 1971, doi: 10.2514/6.1971-380. [Online]. Available: http://arc.aiaa.org

[9] K. W. Garrett and H. M. Rosenberg, "The thermal conductivity of epoxy-resin / powder composite materials," *Journal of Physics D: Applied Physics,* vol. 7, no. 9, pp. 1247-1258, 1974, doi: 10.1088/0022-3727/7/9/311.

[10] J. B. Henderson, W. D. Emmerich, and E. Wassmer, "Measurement of the specific heat and heat of decomposition of a polymer composite to high temperatures," *Journal of Thermal Analysis,* vol. 33, no. 4, pp. 1067-1077, 1988, doi: 10.1007/BF01912731.

[11] D. Noël, J. J. Hechler, K. C. Cole, A. Chouliotis, and K. C. Overbury, "Quantitative thermal characterization of carbon-epoxy composites using differential scanning calorimetry and thermogravimetric analysis," *Thermochimica Acta,* vol. 125, no. C, pp. 191-208, 1988, doi: 10.1016/0040-6031(88)87222-8.

[12] J. G. Quintiere, R. N. Walters, and S. Crowley, "Flammability Properties of Aircraft Carbon-Fiber Structural Composite," Federal Aviation Administration, DOT/FAA/AR-07/57, 2007.

[13] P. Patel *et al.*, "Investigation of the thermal decomposition and flammability of PEEK and its carbon and glass-fibre composites," *Polymer Degradation and Stability,* vol. 96, no. 1, pp. 12-22, 2011, doi: 10.1016/j.polymdegradstab.2010.11.009.

[14] K. Chetehouna, N. Grange, N. Gascoin, L. Lemée, I. Reynaud, and S. Senave, "Release and flammability evaluation of pyrolysis gases from carbon-based composite materials undergoing fire conditions," *Journal of Analytical and Applied Pyrolysis,* vol. 134, pp. 136-142, 2018, doi: 10.1016/j.jaap.2018.06.001.

[15] J. Zhang, M. A. Delichatsios, T. Fateh, M. Suzanne, and S. Ukleja, "Characterization of flammability and fire resistance of carbon fibre reinforced thermoset and thermoplastic

composite materials," *Journal of Loss Prevention in the Process Industries,* vol. 50, pp. 275-282, 2017, doi: 10.1016/j.jlp.2017.10.004.

[16] A. B. Morgan, N. A. Gagliardi, W. A. Price, and M. L. Galaska, "Cone calorimeter testing of S2 glass reinforced polymer composites," *Fire and Materials,* vol. 33, no. 7, pp. 323-344, 2009, doi: 10.1002/fam.995.

[17] T. Fateh, J. Zhang, M. Delichatsios, and T. Rogaume, "Experimental investigation and numerical modelling of the fire performance for epoxy resin carbon fibre composites of variable thicknesses," *Fire and Materials,* vol. 41, no. 4, pp. 307-322, 2017, doi: 10.1002/fam.2381.

[18] D. Quang Dao, J. Luche, F. Richard, T. Rogaume, C. Bourhy-Weber, and S. Ruban, "Determination of characteristic parameters for the thermal decomposition of epoxy resin/carbon fibre composites in cone calorimeter," *International Journal of Hydrogen Energy,* vol. 38, no. 19, pp. 8167-8178, 2013, doi: 10.1016/j.ijhydene.2012.05.116.

[19] C. D. Blasi and I. S. Wichman, "Effects of solid-phase properties on flames spreading over composite materials," *Combustion and Flame,* vol. 102, no. 3, pp. 229-240, 1995, doi: 10.1016/0010-2180(95)00003-O.

[20] A. B. Dodd, B. Shelden, and K. L. Erickson, "Numerical Simulation of Decomposition and Combustion of an Epoxy-Carbon-Fiber Composite," in *Interflam*, Windsor, UK, 2013 2013, pp. 407-412.

[21] N. Régnier and S. Fontaine, "Determination of the thermal degradation kinetic parameters of carbon fibre reinforced epoxy using TG," *Journal of Thermal Analysis and Calorimetry,* vol. 64, no. 2, pp. 789-799, 2001, doi: 10.1023/A:1011512932219.

[22] P. Tadini, N. Grange, K. Chetehouna, N. Gascoin, S. Senave, and I. Reynaud, "Thermal degradation analysis of innovative PEKK-based carbon composites for high-temperature aeronautical components," *Aerospace Science and Technology,* vol. 65, pp. 106-116, 2017, doi: 10.1016/J.AST.2017.02.011.

[23] P. Tranchard, S. Duquesne, F. Samyn, B. Estèbe, and S. Bourbigot, "Kinetic analysis of the thermal decomposition of a carbon fibre-reinforced epoxy resin laminate," *Journal of Analytical and Applied Pyrolysis,* vol. 126, pp. 14-21, 2017, doi: 10.1016/j.jaap.2017.07.002.

[24] M. B. McKinnon, Y. Ding, S. I. Stoliarov, S. Crowley, and R. E. Lyon, "Pyrolysis model for a carbon fiber/epoxy structural aerospace composite," *Journal of Fire Sciences,* vol. 35, no. 1, pp. 36-61, 2017, doi: 10.1177/0734904116679422.

[25] C. Branca, C. Di Blasi, A. Galgano, and E. Milella, "Thermal and kinetic characterization of a toughened epoxy resin reinforced with carbon fibers," *Thermochimica Acta,* vol. 517, no. 1-2, pp. 53-62, 2011, doi: 10.1016/j.tca.2011.01.034.

[26] V. Biasi, G. Leplat, F. Feyel, and P. Beauchêne, "Heat and mass transfers within decomposing carbon fibers/epoxy resin composite materials," in *AIAA Aviation Forum - 11th AIAA/ASME Joing Thermophysics and Heat Transfer Conference*, Atlanta, GA, 2014 2014, doi: 10.2514/6.2014-2678. [Online]. Available: http://arc.aiaa.org

[27] M. Chaos, "Application of sensitivity analyses to condensed-phase pyrolysis modeling," *Fire Safety Journal,* vol. 61, pp. 254-264, 2013, doi: 10.1016/j.firesaf.2013.09.016.

[28] P. Bradna and J. Zima, "Compositional analysis of epoxy matrices of carbon-fibre composites by pyrolysis-gas chromatography/mass spectrometry," *Journal of Analytical and Applied Pyrolysis,* vol. 24, no. 1, pp. 75-85, 1992, doi: 10.1016/0165-2370(92)80006-8.

[29] A. Galgano, C. Di Blasi, C. Branca, and E. Milella, "Thermal response to fire of a fibre-reinforced sandwich panel: Model formulation, selection of intrinsic properties and experimental validation," *Polymer Degradation and Stability,* vol. 94, no. 8, pp. 1267-1280, 2009, doi: 10.1016/j.polymdegradstab.2009.04.007.

[30] N. Grange, K. Chetehouna, N. Gascoin, A. Coppalle, I. Reynaud, and S. Senave, "One-dimensional pyrolysis of carbon based composite materials using FireFOAM," *Fire Safety Journal,* vol. 97, pp. 66-75, 2018, doi: 10.1016/J.FIRESAF.2018.03.002.

[31] P. Krysl, W. T. Ramroth, L. K. Stewart, and R. J. Asaro, "Finite element modelling of fibre reinforced polymer sandwich panels exposed to heat," *International Journal for Numerical Methods in Engineering,* vol. 61, no. 1, pp. 49-68, 2004, doi: 10.1002/nme.1055.

[32] W. Li, H. Huang, and X. Xu, "A coupled thermal/fluid/chemical/ablation method on surface ablation of charring composites," *International Journal of Heat and Mass Transfer,* vol. 109, pp. 725-736, 2017, doi: 10.1016/j.ijheatmasstransfer.2017.02.052.

[33] P. Tranchard, F. Samyn, S. Duquesne, B. Estèbe, and S. Bourbigot, "Modelling Behaviour of a Carbon Epoxy Composite Exposed to Fire: Part I—Characterisation of Thermophysical Properties," *Materials,* vol. 10, no. 5, pp. 494-494, 2017, doi: 10.3390/ma10050494.

[34] P. Tranchard, F. Samyn, S. Duquesne, B. Estèbe, and S. Bourbigot, "Modelling behaviour of a carbon epoxy composite exposed to fire: Part ii-comparison with experimental results," *Materials,* vol. 10, no. 5, 2017, doi: 10.3390/ma10050470.

[35] R. D. Chippendale, I. O. Golosnoy, and P. L. Lewin, "Numerical modelling of thermal decomposition processes and associated damage in carbon fibre composites," *Journal of Physics D: Applied Physics,* vol. 47, no. 38, 2014, doi: 10.1088/0022-3727/47/38/385301.

[36] Y. Guo, Q. Dong, J. Chen, X. Yao, X. Yi, and Y. Jia, "Comparison between temperature and pyrolysis dependent models to evaluate the lightning strike damage of carbon fiber composite laminates," *Composites Part A: Applied Science and Manufacturing,* vol. 97, pp. 10-18, 2017, doi: 10.1016/j.compositesa.2017.02.022.

[37] S. Garcia, J. Guynn, and E. P. Scott, "Use of genetic algorithms in thermal property estimation: Part II - simultaneous estimation of thermal properties," *Numerical Heat Transfer; Part A: Applications,* vol. 33, no. 2, pp. 149-168, 1998, doi: 10.1080/10407789808913932.

[38] A. Dasgupta, R. K. Agarwal, and S. M. Bhandarkar, "Three-dimensional modeling of woven-fabric composites for effective thermo-mechanical and thermal properties," *Composites Science and Technology,* vol. 56, no. 3, pp. 209-223, 1996, doi: 10.1016/0266-3538(95)00111-5.

[39] T. W. Goodrich and B. Y. Lattimer, "Fire decomposition effects on sandwich composite materials," *Composites Part A: Applied Science and Manufacturing,* vol. 43, no. 5, pp. 803-813, 2012, doi: 10.1016/j.compositesa.2011.03.007.

[40] H. Golestanian, "Preform permeability variation with porosity of fiberglass and carbon mats," *Journal of Materials Science,* vol. 43, no. 20, pp. 6676-6681, 2008, doi: 10.1007/s10853-008-2801-0.

[41] J. D. Macias *et al.*, "Thermal Characterization of Carbon Fiber-Reinforced Carbon Composites," *Applied Composite Materials,* vol. 26, no. 1, pp. 321-337, 2019, doi: 10.1007/s10443-018-9694-0.

[42] C. J. Tseng and K. T. Kuo, "Thermal radiative properties of phenolic foam insulation," *Journal of Quantitative Spectroscopy and Radiative Transfer,* vol. 72, no. 4, pp. 349-359, 2002, doi: 10.1016/S0022-4073(01)00129-7.

[43] B. M. Zhang, S. Y. Zhao, and X. D. He, "Experimental and theoretical studies on high-temperature thermal properties of fibrous insulation," *Journal of Quantitative Spectroscopy and Radiative Transfer,* vol. 109, no. 7, pp. 1309-1324, 2008, doi: 10.1016/j.jqsrt.2007.10.008.

[44] A. van Eekelen, L. Ege, and B. J. Lachaud, "Radiation heat-transfer model for the ablation zone of low-density carbon-resin composites," in *10th AIAA/ASME Joint Thermophysics and Heat Transfer Conference*, Chicago, IL, 28 June - 1 July, 2010 2010, doi: 10.2514/6.2010-4904.

[45] L. Pouliot Laforte and L. Laberge Lebel, "Thermal analysis and degradation of properties in carbon fiber/epoxy laminate riveting at high temperatures," *Polymer Testing,* vol. 67, pp. 205-212, 2018, doi: 10.1016/j.polymertesting.2018.02.002.

[46] A. Adibekyan, E. Kononogova, C. Monte, and J. Hollandt, "Review of PTB Measurements on Emissivity, Reflectivity and Transmissivity of Semitransparent Fiber-Reinforced Plastic Composites," *International Journal of Thermophysics,* vol. 40, no. 4, 2019, doi: 10.1007/s10765-019-2498-0.

[47] A. P. Mouritz *et al.*, "Review of fire structural modelling of polymer composites," *Composites Part A: Applied Science and Manufacturing,* vol. 40, no. 12, pp. 1800-1814, 2009, doi: 10.1016/j.compositesa.2009.09.001.

[48] H. L. N. McManus and G. S. Springer, "High Temperature Thermomechanical Behavior of Carbon-Phenolic and Carbon-Carbon Composites, II. Results," *Journal of Composite Materials,* vol. 26, no. 2, pp. 230-255, 1992, doi: 10.1177/002199839202600205.

[49] B. K. Kandola, A. R. Horrocks, P. Myler, and D. Blair, "Mechanical performance of heat/fire damaged novel flame retardant glass-reinforced epoxy composites," *Composites Part A: Applied Science and Manufacturing,* vol. 34, no. 9, pp. 863-873, 2003, doi: 10.1016/S1359-835X(03)00156-8.

[50] Y. I. Dimitrienko, "Thermomechanical behaviour of composite materials and structures under high temperatures: 1. Materials," *Composites Part A: Applied Science and Manufacturing,* vol. 28, no. 5, pp. 453-461, 1997, doi: 10.1016/S1359-835X(96)00144-3.

[51] D. E. Sikoutris, D. E. Vlachos, V. Kostopoulos, S. Jagger, and S. Ledin, "Fire burnthrough response of CFRP aerostructures. Numerical investigation and experimental verification," *Applied Composite Materials,* vol. 19, no. 2, pp. 141-159, 2012, doi: 10.1007/s10443-011-9187-x.

[52] A. P. Mouritz and A. G. Gibson, *Fire Properties of Polymer Composite Materials*. Springer Netherlands, 2006.

[53] A. Frankel, E. Wagman, R. Keedy, B. Houchens, and S. N. Scott, "Embedded-Error Bayesian Calibration of Thermal Decomposition of Organic Materials," *Journal of Verification, Validation and Uncertainty Quantification,* vol. 6, no. 4, 2021, doi: 10.1115/1.4051638.

[54] R. S. P. Hakes Weston-Dawkes, B. Houchens, and S. N. Scott, "Thermogravimetric Analysis (TGA) for Carbon Fiber and Glass Fiber Epoxy Composites and their Constituents," Sandia National Laboritories, Albuquerque, NM USA, 2023, vol. SAND2023-09532.

[55] P. K. Notz, S. R. Subia, M. M. Hopkins, H. K. Moffat, D. R. Noble, and T. O. Okusanya, "SIERRA Multimechanics Module: Aria User Manual," Albuquerque, NM, 2016.

[56] C. Lautenberger and C. Fernandez-Pello, "Generalized pyrolysis model for combustible solids," *Fire Safety Journal,* vol. 44, no. 6, pp. 819-839, 2009, doi: 10.1016/j.firesaf.2009.03.011.

[57] N. Grange, P. Tadini, K. Chetehouna, N. Gascoin, I. Reynaud, and S. Senave, "Determination of thermophysical properties for carbon-reinforced polymer-based composites up to 1000 °C," *Thermochimica Acta,* vol. 659, pp. 157-165, 2018, doi: 10.1016/j.tca.2017.11.014.

[58] R. M. Sullivan, "A Coupled Solution Method for Predicting the Thermostructural Response of Decomposing, Expanding Polymeric Composites," *Journal of Composite Materials,* vol. 27, no. 4, pp. 408-434, 1993, doi: 10.1177/002199839302700404.

[59] H. L. N. McManus and G. S. Springer, "High Temperature Thermomechanical Behavior of Carbon-Phenolic and Carbon-Carbon Composites, I. Analysis," *Journal of Composite Materials,* vol. 26, no. 2, pp. 206-229, 1992, doi: 10.1177/002199839202600204.

DISTRIBUTION

Email—Internal

Name	Org.	Sandia Email Address
Technical Library	1911	sanddocs@sandia.gov

This page left blank

Sandia National Laboratories is a multimission laboratory managed and operated by National Technology & Engineering Solutions of Sandia LLC, a wholly owned subsidiary of Honeywell International Inc. for the U.S. Department of Energy's National Nuclear Security Administration under contract DE-NA0003525.